

Complementary TDCS for the photo-double ionisation of He at 40 eV above threshold in unequal energy sharing conditions

P. Bolognesi¹, R. Camilloni¹, M. Coreno², G. Turri^{2,3,#}, J. Berakdar⁴, A.S. Kheifets⁵ and L. Avaldi¹

¹ CNR-IMAI, Area della Ricerca di Roma, CP10, 00016 Monterotondo Scalo, Italy

² INFN, Laboratorio TASC, Area Science Park, Basovizza, Trieste

³ Dipartimento di Fisica, Politecnico di Milano, Milano

⁴ Max-Planck Institut für Mikrostrukturphysik, Weinberg 2, D-06120 Halle(Saale), Germany

⁵ Research School of Physical Sciences and Engineering, Australian National University, Canberra, ACT 2000, Australia

PACS 32.80

Abstract The photo-double ionisation (PDI) of helium at 40 eV above threshold has been studied for unequal energy sharing conditions in the complementary kinematics obtained by the interchange of the kinetic energies of the two photoelectrons. The triple differential cross sections, TDCS, have been measured in the plane perpendicular to the photon direction using the multicoincidence end-station of the gas phase photoemission beam-line of the Elettra storage ring. The measured TDCS are compared with earlier experimental results obtained in one of the two kinematics studied in this work using a *practical parametrisation* proposed by Cvejanovic and Reddish (J. Phys. B:At. Mol. Opt. Phys. 33 (2000) 4691) and with predictions of the 3C and CCC calculations. A satisfactory agreement between the two sets of experimental data is found. The comparison with the two theoretical models shows that the TDCS in the complementary kinematics still presents a challenge for the theory of PDI.

In photo-double ionisation (PDI) a single incident photon produces two photoelectrons that escape from the residual doubly charged ion core. Due to the single-particle nature of the dipole interaction, the electric field of the photon can act on a single electron only. The transfer of the photon energy to the second electron is then controlled by electronic correlation. A vanishing interaction between the two photoelectrons leads to single photoemission only and hence to a vanishing PDI signal. Thus the PDI is an ideal tool to trace the characteristics of the correlated motion of electronic systems. In the present work we focus on the PDI of helium, which represents the archetype of the three-body Coulomb problem (two interacting electrons coupled to a positive residual ion with no internal structure). The investigation of PDI provides many challenges to both experimentalists and theorists alike. Since the reaction depends upon electron correlations, its total cross section is very small (10^{-21} cm² at 1 eV above threshold [1]). Moreover, a complete characterization of the process implies the detection of the two photoelectrons in coincidence after energy and angular selection. In such an experiment the triply differential cross section $d^3\sigma/d\Omega_1 d\Omega_2 dE_1$ (TDCS), i.e. a cross section differential in the angles of emission of the two photoelectrons $\Omega_1=(\vartheta_1, \varphi_1)$ and $\Omega_2=(\vartheta_2, \varphi_2)$ and in one kinetic energy, is measured. The kinetic energy E_2 of the other electron is determined by energy conservation $h\nu-IP^{2+}=E=E_1+E_2$, where IP^{2+} is the double ionisation potential and E is the excess energy. Thus the low value of the cross section, the need of an energetic and tunable photon source and the intrinsic difficulties of coincidence experiments have hampered the measurements of the TDCS of the PDI process for a long time. On the theoretical side, the correlated motion of the two electrons emerging from the atom has to be described and a proper correlated initial state wavefunction has to be used in order i) to calculate the patterns of the coincidence angular distribution as a function of E and of the energy sharing between the two electrons and ii) to predict the absolute values of the measured TDCS. Considerable progress has been made in the theoretical description of the three-body Coulomb problem, however a universally applicable theory has not been proposed yet.

The first experimental investigation of the PDI in He has been performed by Schwarzkopf *et al.*[2] in 1993 at 20 eV above threshold in equal energy sharing condition ($E_1=E_2$). Since then several measurements have been reported in the literature. They extend from threshold [3,4] up to 80 eV above threshold [5]. The main experimental achievements in the study of two electron

Present address: Western Michigan University and Lawrence Berkeley National Laboratory, ALS Division, 1 Cyclotron Road MS 7-222 Berkeley, CA, USA 94720

processes in the threshold region and the experimental and theoretical results for the PDI of He atom have been recently reviewed [6,7], and will be not repeated here.

By considering the invariance with respect to the rotation around a preferential symmetry axis (for example, the electric vector direction of the incident radiation) and the general properties of the spherical harmonics the TDCS can be written in a way that allows the full separation between the geometrical factors and the dynamical parameters, as shown in a very general way by Briggs and Schmidt[6]. This leads to a parametrisation of the TDCS, first proposed by Huetz *et al.* [8], which is particularly useful for the experimentalists, because it can be easily linked to the experimental observables. In the case of an incident radiation that propagates along the z axis and is linearly polarised along the $\varepsilon=\varepsilon x$ axis the TDCS can be written

$$TDCS(E_1, E_2, \vartheta_{12}) = |a_g(E_1, E_2, \vartheta_{12}) (\cos\vartheta_1 + \cos\vartheta_2) + a_u(E_1, E_2, \vartheta_{12}) (\cos\vartheta_1 - \cos\vartheta_2)|^2 \quad (1)$$

where ϑ_1 and ϑ_2 are the angles of emission of the two photoelectrons with respect to ε and ϑ_{12} is the relative angle between the directions of emission of the two photoelectrons. The complex amplitudes a_g and a_u are respectively symmetric and antisymmetric relative to the exchange of E_1 and E_2 . The ϑ_{12} and E dependence of these amplitudes includes all the physical information on the dynamics of the process, i.e. the effects of the electron-electron and electron-residual ion interactions. Most of the experimental attention has been paid to the study of the TDCS in the case of equal energy sharing. In such a case $a_u=0$, thus the TDCS reduces to a simple form and does not display any circular dichroism [6]. Then the symmetry constraints of the process, expressed by the selection rules [6], reduce the TDCS to a simple shape with characteristic nodes. Several studies of the PDI in equal energy sharing conditions have been reported [3,4,5,6 and references therein]. The main challenge nowadays is to produce absolute values of the TDCS, which can discriminate among different models, which predict similar TDCS patterns, but different magnitudes.

The case of experiments in unequal energy sharing is quite different. In this kinematics both the a_g and a_u amplitudes contribute to the TDCS and effects of circular dichroism are expected to occur for not vanishing circular polarisation of the light [6]. Thus a precise knowledge of the polarisation of the light is vital, unless the radiation of an undulator, which is fully linearly polarised in the odd harmonics, is used. In the case of unequal energy sharing it is instructive to study the complementary TDCS patterns obtained in two experiments by the interchange of the electron kinetic energies, $E_1 \leftrightarrow E_2$. Due to the symmetry properties of a_g and a_u the parametric expression of the TDCS in the two complementary cases will differ by the sign in front of the second addendum of (1). Complementary TDCS have been investigated only from the near threshold region [9,10] up to about 20 eV[10,11] above threshold. Moreover, the predictions of the different theories differ widely amongst themselves when the coincidence angular distribution of the slow electrons with the fast one detected at a fixed direction is considered [6]. Here we present a study of the complementary TDCS for $E=40$ eV and a quite large ratio between the kinetic energies of the two electrons: $E_1 \leftrightarrow E_2 = 5 \text{--} 35$ eV, that correspond to $R = E_2/E_1 = 7$ and $1/7$. In the following the electron measured at a fixed direction will be always labeled as “1”. An excess energy of 40 eV has been chosen because according to previous works [12,6] at this value of the excess energy it may be expected that the single electron behavior dominates over the two-electron correlated emission. In other words, in this region it seems to be reasonable to assume that one electron absorbs the photon and the other one shakes-off in the continuum. This manifests in the U -shape of the energy distribution of the electrons [12] and in the quite different TDCS's depending whether $E_1 < E_2$ or $E_1 > E_2$. Moreover, earlier TDCS measurements at $E_1=5$ eV and $E_2=35$ eV have been reported by the Newcastle group [13]. Combining the two sets of data allows to rule out experimental artifacts and sets the comparison with theory on a more solid ground.

The experiment has been performed at the Gas Phase Photoemission beam-line of the Elettra storage ring. The light source is an undulator of period 12.5 cm, 4.5 m long. The radiation from the undulator is deflected to the variable angle spherical grating monochromator [14] by a prefocusing mirror. The monochromator consists of two optical elements: a plane mirror and a spherical grating. Four interchangeable gratings cover the energy region 20-1000 eV. Two refocusing mirrors after the exit slits provide a circular focus at the interaction region in the multicoincidence end-station [15] used in these experiments. The end-station is lined with a 2

mm thick μ -metal shield. This shield together with coils near the main flanges result in a residual magnetic field less than 10 mG in the experimental chamber. Two independently rotatable turntables are housed in the chamber. Seven spectrometers are mounted at 30° angular intervals on a turntable that rotates in the plane perpendicular to the direction, \mathbf{z} , of propagation of the incident radiation, while three other spectrometers are mounted at 0° , 30° and 60° with respect to polarisation vector ϵ of the light on a smaller turntable. This turntable can be rotated from the perpendicular plane to the (\mathbf{z}, \mathbf{x}) plane. In these measurements both the arrays have been kept in the perpendicular plane.

Each electrostatic spectrometer is composed of four element cylindrical lenses, that focus the photoelectrons from the target region onto the entrance slit of the hemispherical deflector. The mean radius of the hemispherical deflector is 33 mm and the gap is 9.9 mm. In these measurements two rectangular slits of $2 \times 4 \text{ mm}^2$ (2mm is the size of the slit in the dispersion plane) have been used at the entrance and exit of the hemispherical deflector. The energy resolution and the angular acceptance in the dispersion plane of the spectrometers were $\Delta E/E_{1,2}=0.03$ and $\pm 3^\circ$, respectively. This small angular acceptance and the absence of sharp features in the TDCS enables us to compare experiment and theory without any convolution of the latter. Ceramic channeltrons (Dr. Sjuts Optotechnik GmbH) are placed at the exit of the hemispherical deflectors to count the angular and energy selected photoelectrons. The channeltron pulses after being amplified and discriminated are sent to the coincidence electronics, made by three independent time-to-digital converters, TDC. In the experiment each TDC unit is operated in the common start mode with the signal of one of the three analysers of the small turntable used as start and the signals from the other seven as stop. In this way twentyone coincidence pairs are collected simultaneously. The angular distribution is obtained by successive rotations of the larger frame. A PC equipped with a Labview software (National Instruments) sets the voltages of the spectrometers, collects the non coincidence and coincidence data and monitors the flux of the incident beam. The relative efficiency of the spectrometers has been calibrated via the measurement of the photoelectron angular distribution of $\text{He}^+(n=3)$ and of $\text{Kr}^+(3d^{-1})$ at 5 and 35 eV, respectively, above their thresholds. At these energies the β values are known [16,17]. Then the obtained efficiencies have been confirmed by determining the β of the photoelectron angular distribution of $\text{He}^+(1s^{-1})$ at the same kinetic energies. The same efficiency correction has been assumed for the coincidence measurements. The validity of this assumption has been tested by measuring the coincidence yield at two positions of the larger turntable, which allow to overlap two nearby analysers. Therefore all the experimental data are internormalised and can be reported on the same relative scale. This can be checked observing that the same coincidence yield is measured in the case of different configurations of the spectrometers, obtained by the interchange of energies and angles (for example $[E_1=5 \text{ eV}, E_2=35 \text{ eV}, \vartheta_1=30^\circ \text{ and } \vartheta_2=180^\circ]$ and $[E_1=35 \text{ eV}, E_2=5 \text{ eV}, \vartheta_1=0^\circ \text{ and } \vartheta_2=150^\circ]$), which correspond to the same kinematics.

The experiment has been performed at $h\nu=119 \text{ eV}$, using the first harmonic of the undulator. The odd harmonics of the radiation emitted by the undulator are expected to be completely linearly polarised. This has been checked by measuring the photoelectron angular distribution of $\text{He}^+(n=2)$ at the same photon value. A value of the Stokes parameter S_1 of 1 ± 0.03 has been found.

At a photon intensity of 1.4×10^{13} photons/sec (measured by a IRS photodiode placed behind the end-station) and a residual pressure in the chamber of 8×10^{-5} torr typical coincidence rates of 10 mHz per pair of detectors were obtained. The total acquisition time was 10 hours per each complementary kinematics.

The results of the measurements are reported in figures 1a and b, while the differences

$$\begin{aligned} &= TDCS(E_1 = 35 \text{ eV}, E_2 = 5 \text{ eV}) - TDCS(E_1 = 5 \text{ eV}, E_2 = 35 \text{ eV}) \\ &= 4 |a_g| |a_u| \cos \delta (\sin^2 \vartheta_1 - \sin^2 \vartheta_2) \end{aligned}$$

with δ being the relative phase of the amplitudes, are reported in figure 2.

The measurements at $E_1=5 \text{ eV}$ and $\vartheta_1=0$ and 30° (fig.1a) have been performed also by the Newcastle group, see fig. 7 in reference [13] (the angles of ref [13] are related to the present

ones by the relation $180^\circ - \vartheta_1$). When comparing the two sets of experimental TDCS, the angular acceptances, the averaging over different angle segments and the polarisation of the incident radiation have to be accounted for. Thus such a comparison is not straightforward. The shapes of the TDCS measured in the two experiments are in good agreement. The better definition of the minima between the lobes observed in the present measurements and the slight shift of the secondary maxima at $\vartheta_1=0^\circ$ can in part be explained accounting for the different polarisation of the light in the two experiments ($S_1=0.8$ and 1 in [13] and in the present work, respectively). The averaging over 10° segments in both ϑ_1 and ϑ_2 operated on the data collected with the toroidal analyser [13] does not introduce further effects [18]. A more effective comparison between the two sets of data can be done by using a *practical parametrisation* of the TDCS proposed by Cvejanovic and Reddish [19]. This parametrisation, based on the features of the gerade amplitude, relies on the assumption that the angular correlation function is insensitive to the symmetry (gerade ungerade) and to the electron energy sharing. These two factors only affect the ratio between the two amplitudes, $\eta(E,R)$, and their relative phase $\delta(E,R)$. Both the amplitudes are represented by gaussian functions and only three parameters, the correlation width $\vartheta_{1/2}(E)$, $\eta(E,R)$ and $\delta(E,R)$, in the simplest formulation

$$a_g(E, R, \vartheta_{12}) = a_g(E, R=1, \vartheta_{12}) = \exp \frac{-2 \ln 2 (\vartheta_{12} - 180)^\varphi}{\vartheta_{1/2}^2}$$

$$a_u(E, R, \vartheta_{12}) = \eta(E, R) e^{i\delta(E, R)} \exp \frac{-2 \ln 2 (\vartheta_{12} - 180)^\varphi}{\vartheta_{1/2}^2} \quad (2)$$

or four parameters, allowing for different $\vartheta_{1/2}(E)$ in the gerade and ungerade term, are needed in the representation of the TDCS.

The values of the parameters entering Eq. (2) have been obtained in Ref. [19] from a fit to a set of the six TDCS with $E_1=5$ eV ($R=7$) measured previously by the same group [13]. These values are given in Table 1 in comparison with the parameters obtained from the fitting of the present TDCS for $R=7$ and $1/7$.

Table 1

	Ref. [13,19]	This work 3 parameters	This work 4 parameters		CCC	
	Gerade		Gerade	Ungerade	Gerade	Ungerade
$\vartheta_{1/2}(E=40$ eV)	98 ± 1	102 ± 1	104 ± 1	76 ± 2	98	72
$\eta(E=40$ eV, $R=7$)	0.25 ± 0.01	0.25 ± 0.01	0.25 ± 0.01		0.28	
$\delta(E=40$ eV, $R=7$)	$\pm 246^\circ \pm 4^{\text{oa}}$	$\pm 232^\circ \pm 2^{\text{oa}}$	$\pm 229^\circ \pm 2^{\text{oa}}$		243	

^a $\delta(E=40$ eV, $R=7$) = $\delta(E=40$ eV, $R=1/7$) + π [19]

The present values reported in Table 1 are obtained as weighted average among the values produced by fitting the experimental TDCS with Eqs. (1-2). Among all sets of parameters obtained by the fit we found a noticeable difference from the average value in the case of the correlation width of the gerade amplitude for $E_1=5$ eV, $E_2=35$ eV and $\vartheta_1=30^\circ$ where both the 3- or 4-parameter best fits give $\vartheta_{1/2}=93 \pm 3$ and in the case $E_1=35$ eV, $E_2=5$ eV and $\vartheta_1=0^\circ$ where the 3-parameter best fit gives $\delta = \pm 258 \pm 5^\circ$. For sake of clarity only the TDCS obtained from the practical *parametrisation* with 4 parameters are represented in figures 1a and b (full lines) and in the polar plots inserted in the top-left corner of the same figures. Only in the case $E_1=5$ eV, $E_2=35$ eV and $\vartheta_1=30^\circ$ a rescaling factor of 0.88 has been applied to the curves calculated with the average values of the parameters. The results obtained with the 3-parameter fit are comparable, but for the $E_1=35$ eV, $E_2=5$ eV and $\vartheta_1=0^\circ$ where the average value of δ produces a shape in disagreement with the experimental one. The ambiguity in the sign of δ can be resolved

only via the measurement of the complementary TDCS with circularly polarised radiation [6]. As far as the comparison with the data of ref. [19] is concerned, an excellent agreement is found for the width of the correlation function and the ratio η , but the δ value differs by about 15° .

The experiments have been compared with the theoretical predictions of the convergent close coupling (CCC) [20,21] and 3C [22,23] methods.

The CCC methods is a fully numerical approach and relies on intensive computation. For the final state it solves the Schrödinger equation for the system of a photoelectron scattering on the He^+ ion by employing the close coupling expansion of the total wavefunction. The PDI results from the electron impact ionisation of the He^+ ion. The initial state is represented by a highly correlated Hylleraas-type wavefunction. The CCC integrated PDI cross sections agree with the experiment over a broad energy range [21]. Moreover the calculations in the three gauges are practically coincident. Therefore only the velocity gauge calculation is shown in figures 1a and b.

For the sake of comparison the amplitudes a_g and a_u derived from the CCC calculation were fitted with the Gaussian ansatz (2). The fitting parameters are presented in Table 1 along with the values used in the practical parametrization. The two substantially different width parameters are needed to fit the a_g and a_u amplitudes. Both values are consistent with those used in the practical parametrization. The other two parameters η and δ are also close to those obtained from the experiments. Moreover there is no ambiguity in the sign of δ in the CCC calculation.

In the 3C methods an analytical wavefunction where all the interactions in the final state are treated on an equal footing is used [22]. For the initial state a correlated wave function that fulfills the cusp condition has been adopted. The present calculations have been performed in the velocity gauge. In addition to these calculations we also employed the method proposed in ref. [24], which accounts for the two-particle off-shell effects (on the total energy shell). Since the results were only insignificantly different from those obtained within the 3C model we did not include them here.

The experiments have been normalised to the CCC calculation at $E_I=5$ eV, $\vartheta_1=60^\circ$ and $\vartheta_2=300^\circ$. The 3C calculation have been scaled by a factor 0.515 to the CCC one at the same angle. The experimental angular patterns of the TDCS are well reproduced by the two theories. However, in the case of $E_I=5$ eV the theories tend to overestimate the magnitude of the TDCS at $\vartheta_1=30^\circ$ and 0° . The disagreement of the presently measured TDCS with the CCC model can be completely removed by scaling calculation down by a factor of 0.62. We note that a similar factor of 0.88 had to be applied to the practical parametrization to bring it towards the experiment at $\vartheta_1=30^\circ$.

Some discrepancies between the measured TDCS with the 3C calculation are observed. This calculation predicts the positions of the lobe shifted by a few degrees with respect to the experiment at $\vartheta_1 = 60^\circ$ and 30° , and too intense side lobes at $\vartheta_1=0^\circ$. From the understanding of the “practical parametrization” it appears that the size of the side lobes at $\vartheta_1=0^\circ$ are determined by the a_g amplitude. Thus this term seems to be overestimated in the 3C calculation.

In the complementary case a reasonable agreement in the shape of the angular pattern as well as in the relative intensity is observed at $\vartheta_1 = 60^\circ$ and 30° . On the other hand, at $\vartheta_1 = 0^\circ$ different shapes are predicted by the two theories and none of the two agrees with the experimental observation. In this case the practical parameterization gives an acceptable representation of the data, but a change of the relative phase shift δ is needed when only three parameters are used. The angular pattern predicted by the CCC model has some reminiscence of the angular distribution with three lobes of the complementary case, while the one predicted by the 3C model has only one lobe. This latter pattern is expected when the single-electron behavior governs the PDI process. The experiment displays an angular pattern which is better represented by a three lobe structure, although the central feature is not as pronounced as in the CCC calculations. Thus it appears that at $E=40$ eV the PDI process is not yet dominated by the one-electron behavior. This conclusion is in agreement with a recent analysis by Kheifets [25] who showed that correlations become insignificant at excess energies exceeding 100 eV. On the

other hand, if one would make a judgment based solely on the shape of the predicted [12] and measured [26] energy distribution of the photoelectrons, the uncorrelated behaviour could be assumed at this low excess energy of 40 eV. This shows that measurement of the TDCS is a finer tool to disentangle the detail of the PDI process as compared to measurement of the integral or less differential cross sections.

Discrepancies in the measured and calculated shapes of the TDCS for the complementary kinematics at $\vartheta_1 = 0^\circ$ has already been reported in the literature at lower excess energies. Bräuning *et al* [11] noted that the CCC theory predicts the shape of the TDCS which is slightly different from the experiment at $E_1=17$ eV, $E_2=3$ eV and $\vartheta_1 = 0^\circ$. In all other cases studied the CCC theory was consistent with the experiment. On the other hand, the 3C theory was in a good agreement with the experiment at the complementary kinematics at $\vartheta_1 = 0^\circ$ but disagreement was found at $E_1=E_2$ and $E_1=3$ eV, $E_2=17$ eV. Very recently a new calculation by Malegat *et al* [27] confirmed predictions of the CCC theory for the complementary kinematics at $\vartheta_1 = 0^\circ$. So the matter remains controversial.

The comparison of the experimental and theoretical ϑ_2 's in fig.2 confirms the previous observations. The general shape of the difference is well reproduced by the theories at all angles. However at $\vartheta_1=30^\circ$ the CCC model predicts a narrower feature at about $\vartheta_2=250^\circ$ than observed in the experiment, while at $\vartheta_1=0^\circ$ the differences between the 3C calculations and the experiments, already discussed in the description of figures 1a and b, result in higher maxima and deeper minima in figure 2.

In summary, the TDCS of He at 40 eV excess energy have been measured at unequal energy sharing for the complementary cases of $R=7$ and $1/7$ and three different ϑ_1 values. Comparison have been made with the *practical parametrisation* suggested by Cvejanovic and Reddish [19], and the two *ab-initio* theories, the CCC and the 3C. The practical parametrisation with four parameters gives an adequate description of the experiment. The only exception is the kinematics $E_1=5$ eV, $E_2=35$ eV and $\vartheta_1=30^\circ$ where the correlation factor of the gerade amplitude had to be modified and the full curve rescaled by a factor of 0.88. Comparison with the CCC theory is also satisfactory if rescaling is made to different sets of the experimental TDCS. The exception is the complementary kinematics at $\vartheta_1 = 0^\circ$ where the CCC theory predicts much more pronounced maximum in the TDCS at $\vartheta_2 = 180^\circ$. The 3C theory describes qualitatively the main features of the experiment, but disagrees sometime in finer details. Our general conclusion is that the complementary kinematics at a fixed emission direction parallel to the electric vector of the light is the most challenging experimental condition for the theoretical models of the PDI at present.

In addition, our measurement of the TDCS shows that at the excess energy of 40 eV the motion of the two photoelectrons is more correlated than it could be expected solely on the basis of the measurement and calculation of less differential cross sections. This also shows that the transition from the highly correlated motion, typical of the threshold region, to a completely uncorrelated one is a gradual process, which likely ends only asymptotically [23,18].

Acknowledgments

Works partially supported by “INFN-Progetto Luce di Sincrotrone” (Application GAPH002S01). LA gratefully acknowledges stimulating discussions with S. Cvejanovic (who also provided the original data of ref. [13]). The authors thank A. Martin and F. Suran for their help in setting-up the the power supply system of the multicoincidence spectrometers, and M. Mastropietro for the contribution to the development of the counting electronics.

Figure captions

Figure 1: He TDCS for $E=40$ eV , $E_1=5$ eV and $E_2=35$ eV (a) and $E_1=35$ eV and $E_2=5$ eV (b). The experimental TDCS are compared with the predictions of the CCC model (dashed line) and the 3C model (dotted line) in the velocity form and the representation of the TDCS according to the parametrisation of ref.[19] with 4 parameters (full line). The values of the parameters are reported in Table 1 and discussed in the text. In the top-left corner of each panel the experimental data are reported also in polar plots and compared with the results of the parametrisation of ref.[19]. In the case of $E_1=5$ eV and $\vartheta_1=30^\circ$ the results of the parametrisation have been rescaled by 0.88 , while both the 3C and CCC calculations have been rescaled by 0.62 for $E_1=5$ eV and $\vartheta_1=30^\circ$ and 0° .

Figure 2: The differences between the complementary TDCS, σ_{comp} , are compared with the theoretical ones (dashed line: CCC length form, dotted line : 3C velocity form) and the ones obtained from the representation of the TDCS according the parametrisation of ref. [19] with 4 parameters (full line).

Table explanation

Table 1: The values of the α , β and γ parameters as obtained by a fit of the present data (see text) and in ref. [19] for the kinematics with $E_1=5$ eV ($R=7$) are shown. In the last column the values obtained by fitting the parametric expression of the amplitudes to the CCC calculation are reported.

Figure 1a

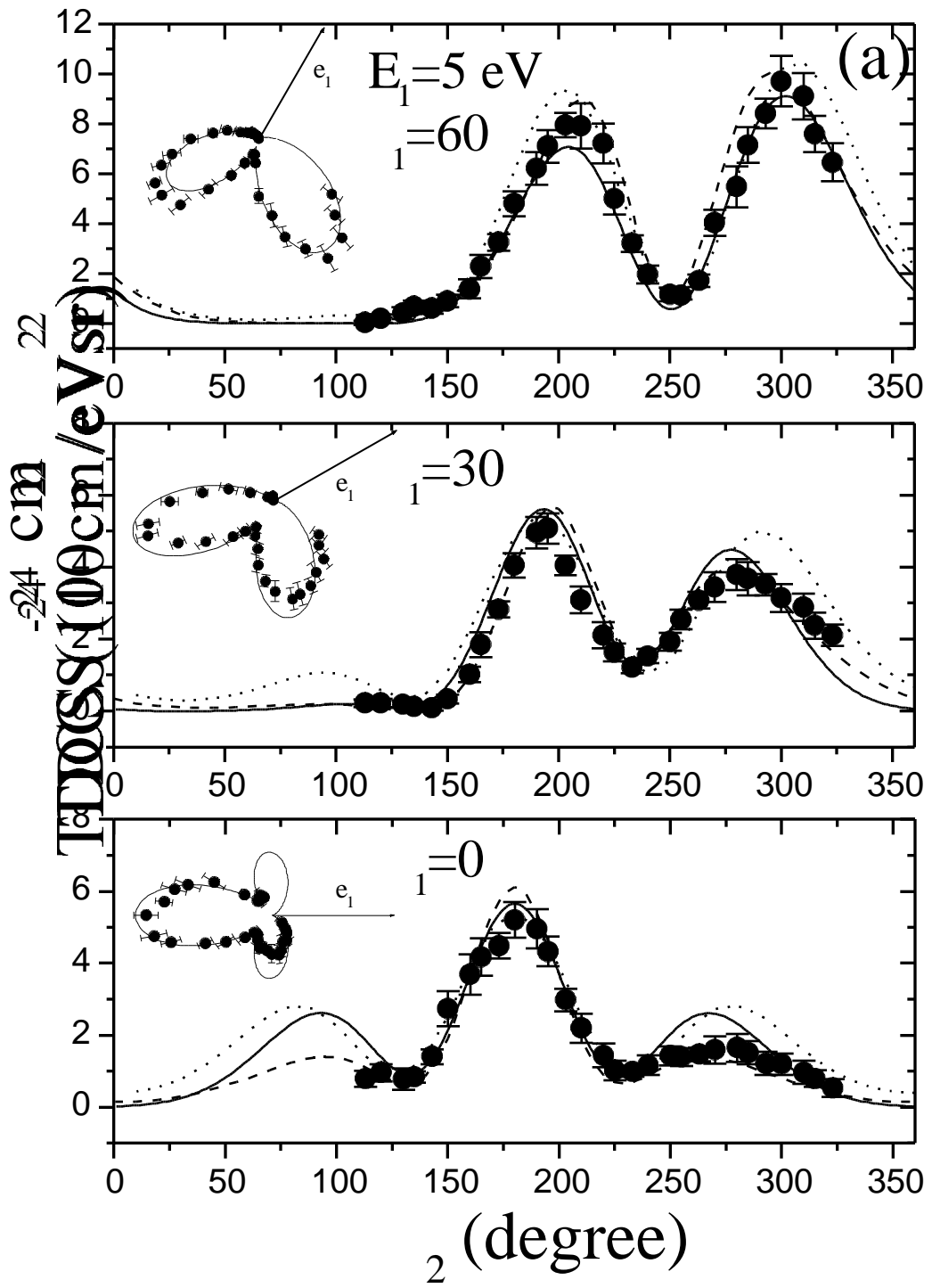


Figure 1b

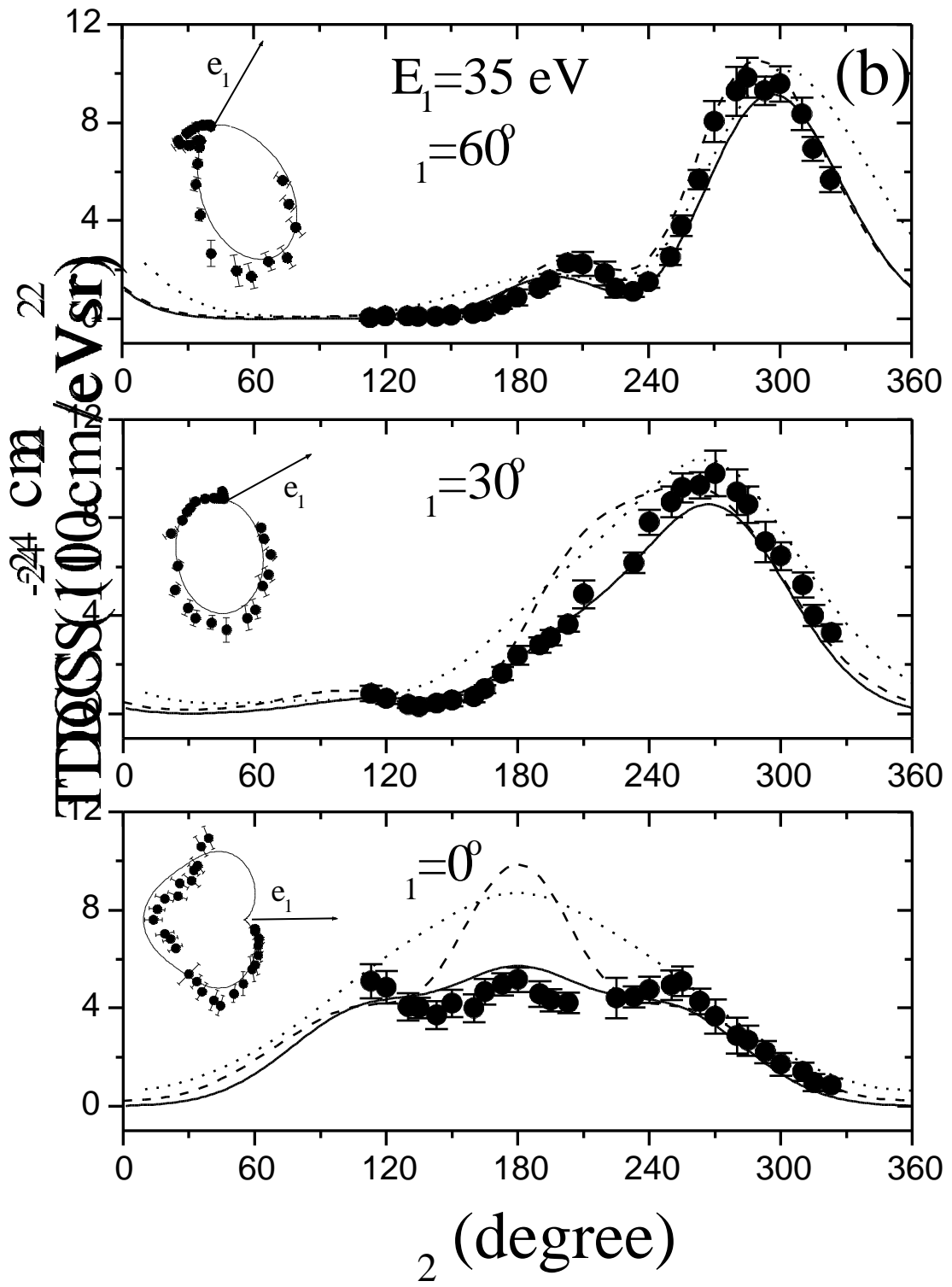
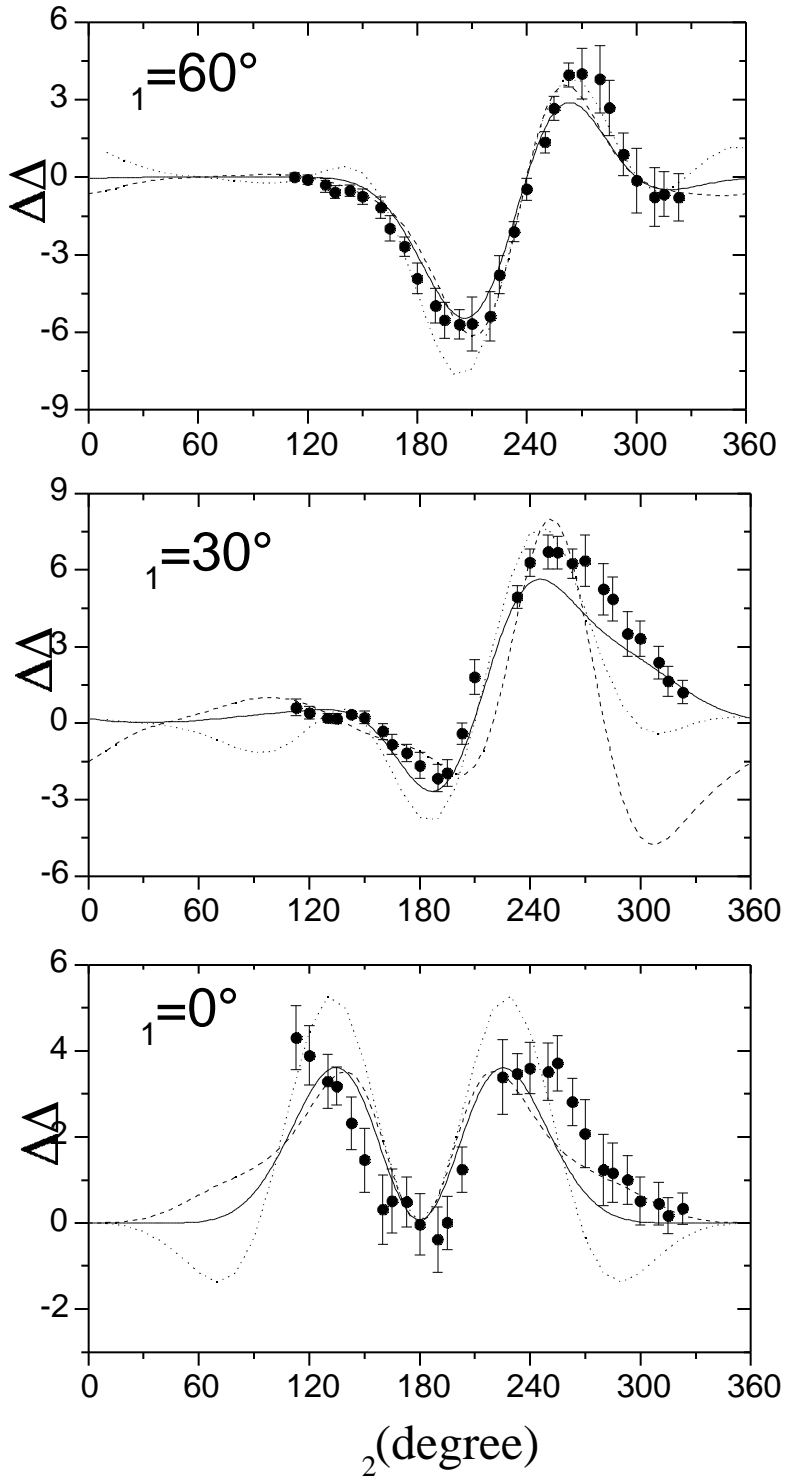


Figure 2



References

- 1 Kossmann H, Schmidt V and Andersen T 1988 Phys. Rev. Lett. **58** 1620
- 2 Schwarzkopf O, Krässig B, Elminger J and Schmidt V 1993 Phys. Rev. Lett. **70** 3008
- 3 Huetz A and Mazeau J 2000 Phys. Rev. Lett. **85** 530
- 4 Gulley N 1997 PhD Thesis University of Manchester
- 5 Avaldi L., Battera G, Camilloni R, Coreno M, DeSimone M, Prince K C, Turri G, Zitnik M and Stefani G 2000 XXI- ICPEAC, Book of Abstracts, Itikawa et al. Ed.s, p23
- 6 Briggs J S and Schmidt V 2000 J. Phys. B:At. Mol. Opt. Phys. **33** R1
- 7 King G C and Avaldi L 2000 J. Phys. B:At. Mol. Opt. Phys. **33** R215
- 8 Huetz A, Selles P, Waymel D and Mazeau J 1991 J. Phys. B:At. Mol. Opt. Phys. **24** 1917
- 9 Dawber G, Avaldi L, McConkey A G, Rojas H, MacDonald M A and King G C 1995 J. Phys. B:At. Mol. Opt. Phys. **28** L271
- 10 Lablanquie P, Mazeau J, Andric L, Selles P and Huetz A 1995 Phys. Rev. Lett. **74** 2192
- 11 Bräuning H, Dörner, Cocke C L, Prior M H, Krässig B, Kheifets A S, Bray I, Bräuning-Demian A, Carnes K, Dreuil S, Mergel V, Richard P, Ullrich J and Schmidt-Böcking H 1998 J. Phys. B:At. Mol. Opt. Phys. **31** 5149
- 12 Proulx D and Shakeshaft R 1993 Phys. Rev. A **48** R875
- 13 Cvejanovic S, Wightman J P, Reddish T J, Maulbetsch F, MacDonald M A, Kheifets A S and Bray I 2000 J. Phys. B:At. Mol. Opt. Phys. **33** 265
- 14 Melpignano P, Di Fonzo S, Bianco A and Jark W 1995 Rev. Sci. Instrum. **66** 2125
- 15 Blyth R R, Delaunay R, Zitnik M, Krempasky J, Krempaska R, Slezak J, Prince K C, Richter R, Vondracek M, Camilloni R, Avaldi L, Coreno M, Stefani G, Furlani C, DeSimone M, Stranges S and Adam M-Y 1999 J. Electron Spectrosc. Relat. Phenom. **101-103** 959
- 16 Wehlitz R, Langer B, Berrah N, Whitfield S B, Viehhaus J and Becker U 1993 J. Phys. B: At. Mol. Opt. Phys. **26** L783
- 17 Lindle D W, Heiman P A, Ferret T A, Kobrin P H, Truesdale C M, Becker U, Kerkhoff H G and Shirley D A 1986 Phys. Rev. A **33** 319
- 18 Cvejanovic 2001 private communication
- 19 Cvejanovic S and Reddish T J 2000 J. Phys. B:At. Mol. Opt. Phys. **33** 4691
- 20 Kheifets A S and Bray I 1998 J. Phys. B:At. Mol. Opt. Phys. **31** L447; Phys. Rev. Lett. **81** 4588
- 21 Kheifets A S and Bray I 1998 Phys. Rev. A **58** 4501
- 22 Bräuner M, Briggs J S and Klar H 1989 J. Phys. B:At. Mol. Opt. Phys. **22** 2265
- 23 Maulbetsch F and Briggs J S 1994 J. Phys. B:At. Mol. Opt. Phys. **27** 4095
- 24 Berakdar J 1997 Phys. Rev. Lett. **78**, 2712
- 25 Kheifets AS 2001 J. Phys. B:At. Mol. Opt. Phys. **34**, L247
- 26 Wehlitz R, Heiser F, Hemmers O, Langer B, Menzel A and Becker U 1991 Phys. Rev. Lett. **67** 3764
- 26 Malegat L, Selles P and Kazansky AK, 2000 Phys. Rev. Lett. **85** 4450